Robust Fuzzy C-Means Clustering Algorithm Based on Normal Shrink and Membership Filtering for Image Segmentation

Tunirani Nayak
Department of Electronics and Telecommunication Engineering.,
VSSUT, Burla, Sambalpur,768018, Odisha,India
tnayak_eltc@vssut.ac.in

and

Nilamani Bhoi
Department of Electronics and Telecommunication Engineering.,
VSSUT, Burla, Sambalpur,768018, Odisha,India
nbhoi_etc@vssut.ac.in

Abstract

The robustness and effectiveness of image segmentation using the FCM algorithm can be improved by incorporating local spatial information into the FCM method, which is particularly noise-tolerant. However, the introduction of local spatial information gives more computational complexity. Hence to overcome this problem an improved FCM clustering method is proposed which is based on a normal shrink algorithm with membership filtering. The Proposed method gives a faster and more robust result in comparison to FCM. Firstly, a normal shrink denoising algorithm is introduced to preserve the image details and noise immunity. Secondly, membership filtering is introduced, which depends only on the local spatial neighboring properties of the matrix called the membership partition matrix. The Proposed method is faster and simpler as it does not calculate the distance between pixels and cluster centers and between local spatial neighboring. Also, it is very efficient for noise immunity.

Keywords- Image Segmentation, FCM, normal shrink denoising algorithm, membership filtering

1 Introduction

Image segmentation, with its resilience and variety of applications, is one of the most difficult and creative fields in the study of computer vision. An image is separated into its non-overlapping constituent areas during image segmentation [1][2]. A greater variety of image segmentation techniques were proposed by many scientists. Region growing [3], watershed transform [4], clustering [5], mean shift [6], graph cut [7], neural network [9], markov random field [8], and other methods and technologies are examples of image segmentation techniques. Due to its stability for image segmentation, clustering is a very useful and popular approach in the present day. Clustering techniques fall into several types, including graph-based, hierarchical, density function-based, and objective function minimization-based techniques.

Bezdek [10] suggested FCM, a gentle clustering approach. FCM is more resilient than the hard clustering approach, is more ambiguity-tolerant, and securely keeps the data in an image. However, if we look at the FCM algorithm's shortcomings, we find that it is unable to segment an image that has been tainted by any kind of noise and has a complicated texture since it only takes into account grey levels and ignores spatial information. FCM_S was suggested by Ahmed et al. [11] as a solution to this issue. In this method, the intensity inhomogeneity is considered to account and also the pixel. In the method, FCM_S, the time of execution is more because the spatial information of the neighborhood is computed in each step of the iteration process. FCM_S1 and FCM_S2 were proposed by Chen and Zhang [12], to compute the spatial information of the neighborhood in advance. Both these filters are not prone to Gaussian noise. These two methods have lower computational costs than FCM_S because, before the iterative stage, the filtered images can be computed using a median and mean filter. To identify the noise types, present in an image, intensity Enhanced-FCM(EnFCM) [13] has been proposed. It is a very efficient algorithm because it uses very low computational time. Here the clustering is based on the gray level of an image. The drawback of the EnFCM is, the segmented output is only comparable with the output of FCM_S. To overcome this Cai et al. [14] proposed another advanced algorithm called fast generalized FCM (FGFCM). Here clustering is performed over a gray-level histogram. It is more robust and computationally efficient than EnFCM.

The next advanced FCM algorithm is FLICM which was proposed by Krinidis and Chatzis [15]. The objective function of FLICM give guaranteed image details preservation and noise immunity. Although it has improved the segmentation efficiency, it does not give a robust spatial distance. Gong et al [16] proposed an algorithm called RFLICM, which is another variant of FLICM. It emphasizes local context information of images with a variable spatial distance. To enhance the effectiveness of the clustering algorithm, a kernel metric is introduced. Gong et al. [17] proposed a new fuzzy c-means clustering based on kernel metric and local information called (KWFLICM). Although it is a parameter-free selection method, it gives more computational complexity.

The major challenges faced by fuzzy clustering algorithms are as follows.

(i)The fuzzy clustering algorithm fails to perform segmentation tasks in noisy conditions.

(ii) It fails to remove the misclassified pixels.

To overcome these issues, the Proposed method is proposed.

The following is a summary of our primary contributions:

The Proposed method circumvents the challenge of selecting alternative filters appropriate for various kinds of noise in the current enhanced FCM algorithms by using normal shrink (NS) as pre-processing stages to eliminate any noise and maintain image features. The Proposed approach is therefore more reliable for images corrupted by various kinds of noise than these algorithms[12][13][14][15][16][17].

In the Proposed method, the distance between pixels inside local spatial neighbors and their clustering centers is computed more slowly using membership filtering, hence altering the membership partition. As a result, compared to existing enhanced FCM algorithms [11][12][13][14][15], the Proposed method is faster.

The organization of this paper is presented as follows. In Section 1 introduction is described. In Section 2 motivation is presented. In Section 3 we introduce the methodology for image segmentation. Section 4 describes the images and ground truth. Section 5 describes the performance measures. In Section 6 we describe the experimental result and discussion. The advantages and limitations of the proposed method is highlighted in Section 7. Finally, we provide a conclusion in Section 8.

2 Motivation

Many researchers developed many algorithms considering noise immunity. To minimize the FCM algorithm's flaw, which is that it is extremely noise-sensitive, most of the scientists approached many methods such as FLICM, NWFCM, etc, here local spatial information is applied to FCM. Here the performance of the FCM algorithm is improved in different ways, initially, a novel technique is used to introduce local spatial information that requires less time, and computing complexity, and secondly modify the membership matrix.

2.1 Motivation for using normal shrink denoising algorithm

FCM gives poor performance for image segmentation with highly noise-sensitive and other imaging effects. In the literature review, many researchers have proposed many methods to modify FCM to make it more stable by considering both noise and complexity. Hence the performance can be satisfactory for severely noisy images. The improved version of the FCM algorithm is noise-resistant, and hence the performance is good for any type of image segmentation.

In FCM [10] the cluster centre u is fixed and set manually. In order to handle the noisy pixels, the original FCM algorithm is modified [18].

Generally, the modified objective function of the FCM algorithm is given as follows:

$$J_n = \sum_{i=1}^{N}\sum_{k=1}^{u} w_{ki}^{n} \|f_i - z_k\|^2 + \sum_{i=1}^{N}\sum_{k=1}^{u} M_{ki} \quad (1)$$

Where f = {f_1, f_2, …….,f_N} represents a gray scale image,, z_k is the type of value of k^{th} cluster, f_i is the ith gray value of the pixels, w_{ki} is the fuzzy membership value of the ith pixel of cluster k. The number of clusters is equal to u, whereas the total number of pixels in an image is N. Weighing the exponent parameter n provides a description of the degree of fuzziness of the final categorization. The parameter M_{ki} is a fuzzy control parameter that determines the computational cost of various algorithms as well as how the neighborhood pixel is controlled in relation to the central pixel.

FCM_S1 and FCM_S2 have the simplest form of M_{ki} than FCM_S. As FCM_S1 and FCM_S2 provide very good segmentation results, finding a noise type that is necessary to select an appropriate denoising method is challenging.FCM_S2 fails to segment for Gaussian noise but gives a very good result for salt & pepper noise. We try to preserve neighbouring pixel details or image details by efficiently removing different types of noises. Due to this motivation, we introduce the normal shrink denoising algorithm to FCM because it eliminates any type of noise in comparison to any type of conventional filter. Hence image details are preserved for image segmentation.

Here, we compare the effectiveness of the normal shrink-denoising algorithm on the dataset and real images. The normal shrink denoising algorithm is compared with the mean and median filter. The performance is measured with PSNR values. In our Proposed method, initially, the robustness of the images is tested by adding Gaussian noise and salt & pepper noise. We got the corrupted image. Also, for more useful applications, we provide mixed noise, which combines Gaussian noise with salt & pepper noise and has a zero mean and a distinct variance. The PSNR values have been calculated. From Table 1 and Table 2, it is shown that the PSNR values are very high in the normal shrink denoising algorithm for different values of variance. Here we are using MATLAB 18 for processing of images. The noise variance is 5%,10%,15%,20%,25%,30% and 40%. But our result as shown in Figure 1 and Figure 3 is based on 15% variance. Figure 1 is the processing of Lena text image and Figure 3 is the processing of the Bird image from the Weizman dataset. Figure 2 and Figure 4 show the graphical representation of PSNR values with different variances. As shown in the figures the mean and median filters graph is overlap because of nearly equal PSNR values.

(a) (b) (c) (d) (e)

Figure 1: Comparison of different methods (15% variance) (a) Lena image (b) noisy image (c) output image using mean filtering(d) output image using median filtering(e) output image using normal shrink

Table 1: PSNR values of Mean, Median, and normal shrink denoising method with mixed noise			
Noise	Mean filter	Median filter	Normal Shrink
5%	15.8817	15.8354	17.2011
10%	13.3349	13.3874	15.1800
15%	11.5773	11.5875	13.7821
20%	10.2187	10.2221	12.6267
25%	9.1425	9.1527	11.6951
30%	8.2860	8.2866	10.9064
40%	7.0247	7.0367	9.5890

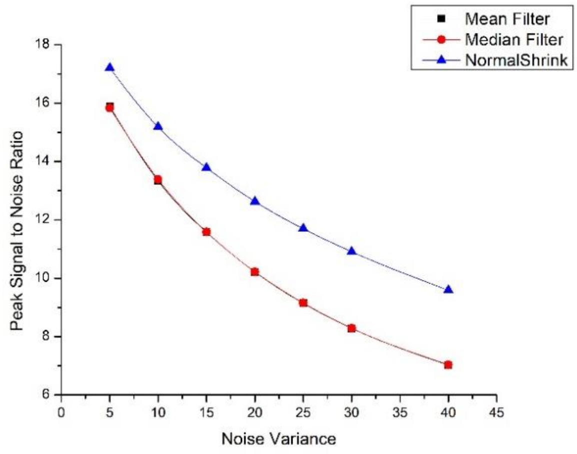

Figure 2: Comparison of PSNR values of Mean filter, Median filter, and normal shrink denoising method of Lena text image.

(a) (b) (c) (d) (e)

Figure 3: Comparison of different methods (15% variance). (a) Bird dataset image (b) noisy image(c) output image using mean filtering(d) output image using median filtering(e) output image using normal shrink

Table 2: PSNR values of Mean, Median, and Normal Shrink with mixed noise			
Noise	Mean filter	Median filter	Normal shrink
5%	15.7465	15.7557	16.9075
10%	13.2217	13.2228	14.8205
15%	11.5513	11.6112	13.2230
20%	10.2912	10.3216	12.0168
25%	9.3572	9.3421	11.0848
30%	8.6016	8.5555	10.3685
40%	7.5264	7.5177	9.1898

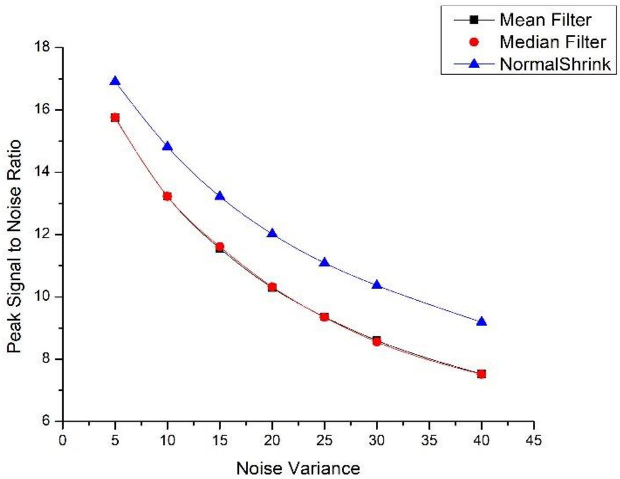

Figure 4: Comparison of PSNR values of mean filter, median filter, and normal shrink denoising method of 0223 dataset image.

2.2 Motivation for using Membership Filtering

According to the modified objective function defined in the FCM algorithm [18] and using the Lagrange multiplier method [18], the membership partition matrix is given as

$$w_{ki} = \frac{\|f_i - z_k\|^{-2/(n-1)}}{\sum_{j=1}^{u} \|f_i - z_j\|^{-2/(n-1)}} \tag{2}$$

And the clustering center is given as

$$z_k = \frac{\sum_{i=1}^{N} w_{ki}^n f_i}{\sum_{i=1}^{N} w_{ki}^n} \tag{3}$$

According to (2), it is easy to calculate the membership partition matrix u_{ki}, but when we modified and improved the FCM algorithm such as FLICM and KWFLICM, it is very slow and complex. And also, it increases the computational complexity. Again, if we want to introduce the fuzzy factor M_{ki} , it is more robust for image segmentation of noisy images but the computational cost is increased. Hence it is a difficult task how to decrease the computational complexity and increase the robustness simultaneously for FCM.

In order to resolve the discrepancy described above, membership filtering is here added to FCM. Initial clustering is done on the histogram of a denoised image since we have the denoised image beforehand. After getting a fuzzy membership partition matrix, the membership matrix is modified using membership filtering. This takes place to reduce the difficulty of calculating the distance between adjacent pixels and cluster centers.

3 Methodology

Here the image segmentation was performed with the following steps. Initially, we replace the mean or median filter with a normal shrink-denoising algorithm, because it is more immune to noise. A normal shrink algorithm can suppress any type of noise without considering the noise type. We got a new image from a normal shrink algorithm. The gray-level histogram was obtained from the new image. Then fuzzy membership matrix was obtained from the clustering method applied over the gray-level histogram of an image and the idea was motivated by the EnFCM algorithm. Finally, a membership filter is selected to obtain a modified membership matrix. In this method, a very good output segmentation result was obtained.

Block diagram of the Proposed method

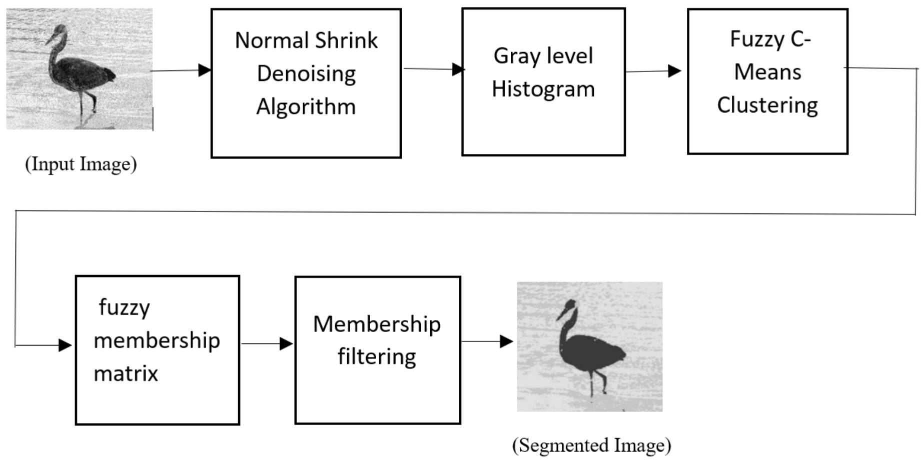

Figure 5: Block Diagram of the Proposed method

3.1 Normal Shrinking Algorithm

In the FCM algorithm, the convergence factor depends on the data distributed in the cluster. If it successfully forms a cluster, then the iteration number is less. Since noise always affects the cluster data, FCM is one of the approaches that is always susceptible to it. Due to these two types of problems arise, the first one is that the segmentation outcome in the case of a noisy image is poor and the second one is the number of iterations is more in the case of a noisy image than the image is not corrupted by noise. To consider both noisy and uncorrupted images by noise, the histogram is the most effective tool for describing how data are distributed. In the case of the uniform histogram, the segmentation outcome is not accurate and quick. The result is good in case of the histogram has several peaks.

Figure 6 shows the histogram of the original image. MATLAB 18 is used to find out the histogram of Lena image.

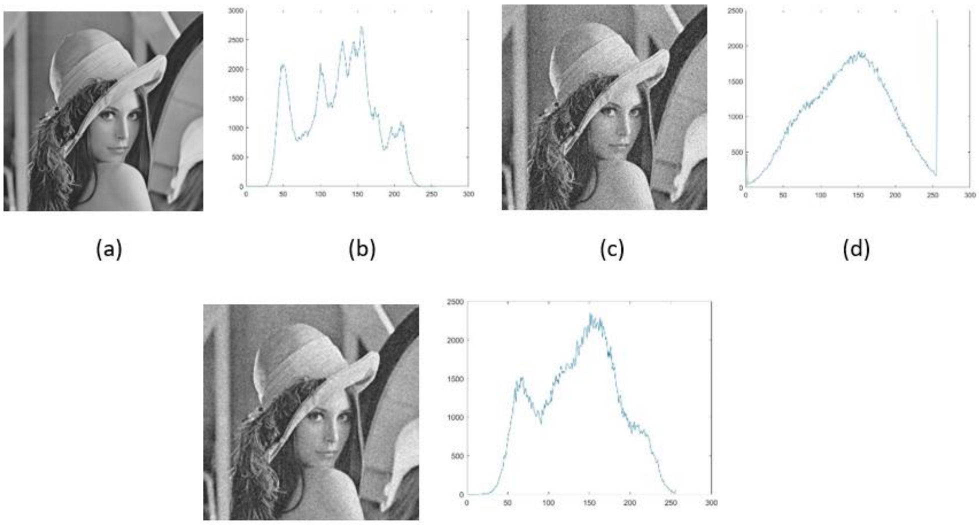

(a) (b) (c) (d)

(e) (f)

Figure 6: (a) original image Lena (image size: 512x512) (b) histogram of Lena image. (c) noisy image (Gaussian noise with zero mean and variance is 5%). (d) histogram of (c). (e) filtered image (mean filter (3x3)). (f) histogram of (e).

As per Figure 6(b), in the histogram of the original image, there are multiple numbers of peaks, but there is no peak in the histogram of the noisy image (by Gaussian noise) according to Figure 6(d). Two peaks are only in Figure 6(f) which is the output of the mean filter. Hence it concluded that Gaussian noise can be reduced efficiently by a mean filter. (Filtered window size is 3x3). For Gaussian noise removal, one of the efficient filters is the mean filter, because the data distribution is optimized. Hence the iteration is less.

Here we introduced a normal shrink-denoising algorithm [19] for noise removal, which removes the noise, without knowing the type of noise added to the image. Image denoising is one of the most important and challenging methods for noise removal. Two approaches are used for image denoising, one is the wavelet approach and the other is the non-wavelet approach. Here we are using the wavelet approach. One of the most common wavelet approaches and selection of thresholds is wavelet shrinkage. To get a faster convergence, normal shrink performance is faster than others because the processing time is faster than other methods.

The original image obtained by this algorithm is given by:

$$g(x,y) = \frac{1}{\sqrt{UV}}\sum_u \sum_v W_\varphi(j_0,u,v)\ \varphi_{j0,u,v}(x,y) + \frac{1}{\sqrt{UV}}\sum_{i=H,V,D}\sum_{j=j0}^{\infty}\sum_u\sum_v {W^i}_\Psi(j,u,v)\Psi^i_{j,u,v}(x,y) \qquad (4)$$

Where $g(x,y)$ is the original image, the $W_\varphi(j_0,u,v)$ coefficient defines an approximation of noisy $g'(x,y)$ at scale j_0. The ${W^i}_\Psi(j,u,v)$ coefficients add horizontal, vertical, and diagonal details for scales $j \leq j_0$. The $\varphi_{j0,u,v}(x,y)$ is scaled basis function and the $\Psi^i_{j,u,v}(x,y)$ is the translated basis function.

Figure 7 shows different noise removal output images and the comparison with the normal shrink. The original image is shown in Figure 7(a). Here the filter size taken for a mean and median filter is 3x3.

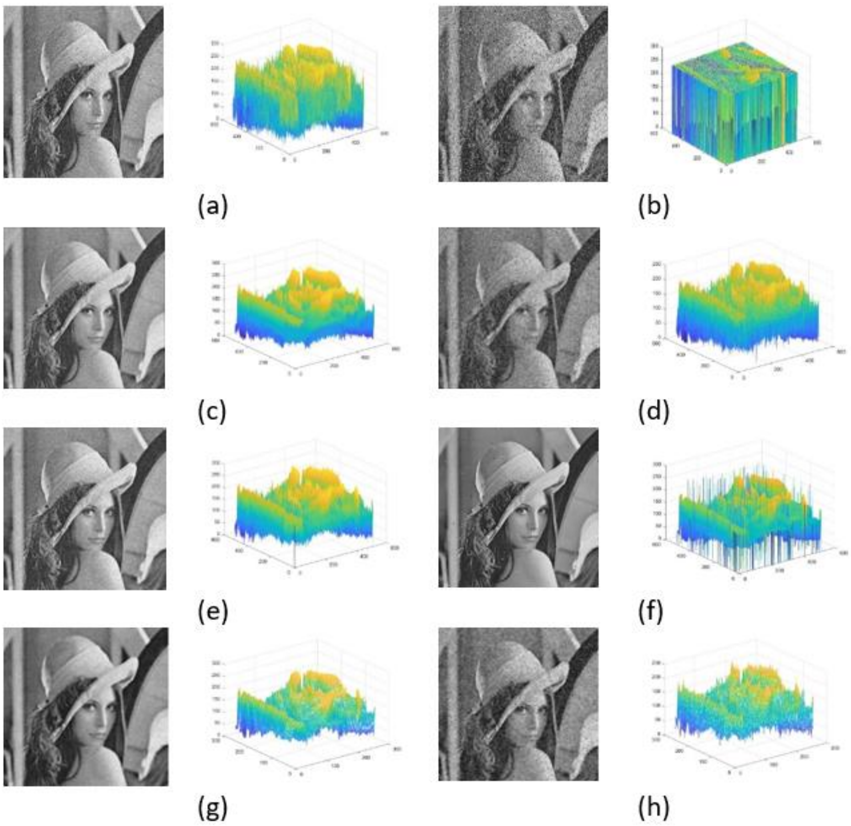

Figure 7: Comparison of different noise removal methods over Lena text image. (a) corrupted image (Gaussian noise with zero means and 5% variance). (b) corrupted image (salt & pepper noise with 20% variance). (c) mean filtering result for (a). (d) mean filtering output result for (b). (e) median filtering result for (a). (f) median filtering output result for (b). (g) normal shrink result for (a). (h) normal shrink result for (b).

Figure 7 compares the output produced by a median filter, a mean filter, and normal shrink in order to demonstrate the impact of normal shrink for various types of noise reduction in images. The mean, median, and normal shrink techniques are used to filter the Gaussian noise-corrupted image as shown in Figure 7(c, e, g). Comparably, the mean filter, median filter, and normal shrink are used in Figure 7(d, f, h) to filter images corrupted by salt & pepper noise. According to the above observation, Gaussian noise and salt & pepper noise may both be effectively eliminated using normal shrink. Without taking into account the type of noise, normal shrink is likewise capable of optimizing the data. Overall normal shrink gives a good result in comparison to the mean and median filters. The denoised image is given below.

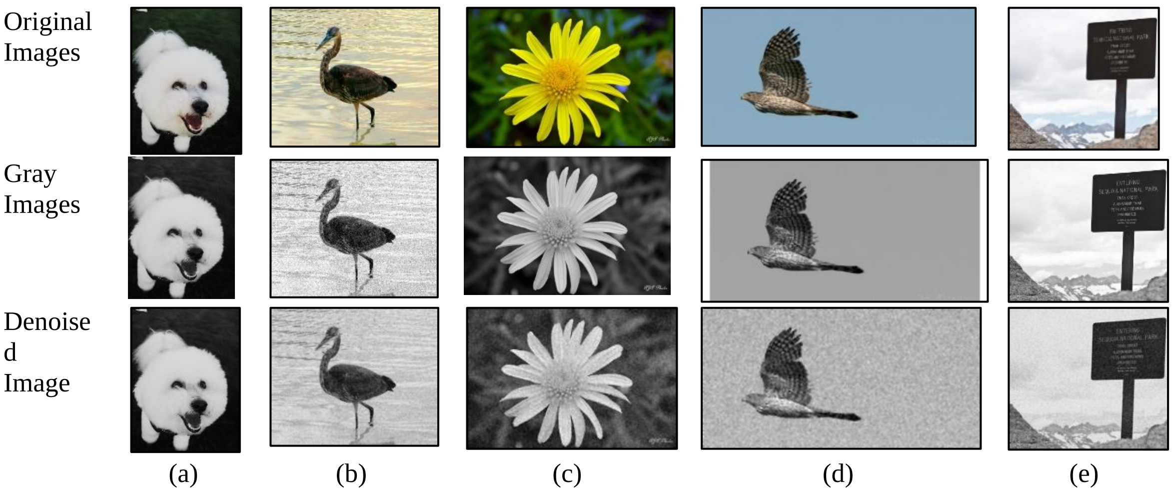

Figure 8: Output result of normal shrink denoising algorithm

3.2 Membership Filtering

Adding a fuzzy element to the objective function can increase the FCM algorithm's effectiveness. Consideration is given to the fuzzy factor, which is often utilized to limit the impact of neighbouring pixels on the center pixel. Hence different variation of fuzzy factors leads to deriving FCM_S, FLICM, FCM-S1, FCM-S2, etc. But because of this fuzzy factor, computational complexity is increased. Hence it is very difficult to reduce the complexity and increase the robustness simultaneously in FCM.

Hence it was proposed membership filtering to FCM. Firstly, a denoised image is created in advance. Secondly, the histogram was obtained from the denoised image, and the clustering was applied to the histogram. We are getting a membership partition matrix based on fuzzy. Here membership filtering is used over the membership partition matrix to modify it and to prevent the estimated distance between the cluster centre and the adjacent pixel. Also, membership filtering has the capability of correcting pixels that are misclassified. Hence it is a good choice to use the membership filter rather than a fuzzy factor in the objective function. Hence FCM algorithm will converge quickly with membership filtering.

170	170	170
170	170	170
170	170	170

(a)

165	110	125
175	190	145
158	220	175

(b)

0.02	0.01	0.02
0.01	0.00	0.03
0.01	0.02	0.01

0.10	0.96	0.80
0.03	0.00	0.40
0.02	0.05	0.03

0.82	0.01	0.12
0.93	1.00	0.52
0.62	0.93	0.98

(c)

0.01	0.02	0.01
0.01	0.00	0.04
0.03	0.01	0.01

0.05	0.06	0.09
0.03	0.03	0.12
0.02	0.05	0.03

0.87	0.90	0.87
0.93	0.95	0.76
0.88	0.95	0.94

(d)

Figure 9: Comparison of the FCM algorithm's partition matrices and FCM based on membership filter (u=3 with a step of 10 iteration). (a) The original synthetic image has three gray levels (0,87,170). (b) Gaussian noise-corrupted image (zero mean, and 5% variance). (c) Membership partition using FCM. (d) Using FCM for membership partitioning based on membership filter for (c).

Figure 9 shows how membership partition is affected by spatial neighborhood information. Some misclassified pixels are shown in Figure 9(c). For a pixel (the gray value is 110) in Figure 9(b), we obtained three fuzzy memberships (0.01,0.96,0.01) of the pixel shown in Figure 9(c) by using FCM, which clearly demonstrates that, in accordance with FCM, the pixel belongs to the second cluster. But in actuality, the Ground Truth indicates that it is a part of the third cluster (the gray value is 170). Membership filtering is capable of rectifying misclassified pixels, as seen in Figure 9(d). Consequently, it makes sense to apply membership filtering rather than adding fuzzy factors. M_{ki}. Furthermore, compared to FCM, the membership filtering-based FCM method (MFFCM) produces superior clustering centers.

The overall algorithm is summarized below:

a. Initialize the number of clusters and the size of the filtering window.

b. Compute the new image using the normal shrink algorithm and compute the histogram of the new image

c. The membership partition matrix is calculated from the histogram of the gray image

d. The membership partition image is modified by membership filtering.

e. Finally median filtering is applied to speed up the algorithm.

4 The images and ground truth

For image clustering, a variety of photos have been pulled from the Weizmann dataset. Depending on whether the foreground and background are plain or textured, there are many image classifications. The kinds of images employed in segmentation is Dog, Bird, Flower, Eagle, and Board are shown in Fig. 10.

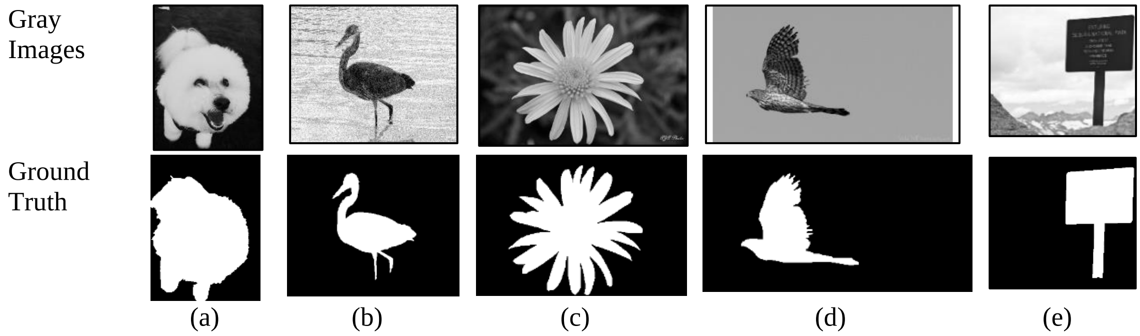

Figure 10: Different images are (a) Dog (b) Bird (c) Flower (d) Eagle (e) Board

5 Performance measures

The segmentation output of the Proposed method is compared with the real image to determine how effective the offered strategy is. Performance metrics including accuracy, sensitivity, F-measure, precision, MCC, dice, Jaccard, and specificity are used to compare the recommended technique's performance to the existing approach. The formula for different performance metrics is given in Table 3.

True Positive (TP): Intersection of segmented output foreground pixel and ground truth.

False Positive (FP): Intersection of segmented output foreground pixel and pixels in the background of ground truth.

True Negative (TN): Intersection of segmented output background pixel and ground truth.

False Negative (FN): Intersection of segmented output background pixel and pixels in the foreground of ground truth.

Table 3: The formula of different parameters

Sl.No	Parameters	Formula
1	Accuracy	$\frac{(TP+TN)}{(FN+FP+TP+TN)}$
2	Sensitivity	$\frac{(TP)}{(TP+FN)}$
3	Precision	$\frac{(TP)}{(TP+FP)}$
4	F-measure	$\frac{(2\times TP)}{(2\times TP+FP+FN)}$
5	MCC	$\frac{(TP\times TN)-(FP\times FN)}{\sqrt{(TP+FP)\times(TP+FN)\times(TN+FP)\times(TN+FN)}}$
6	Dice	$\frac{2\times TP}{(2\times TP+FP+FN)}$
7	Jaccard	$\frac{Dice}{(2-Dice)}$
8	Specificity	$\frac{TN}{(TP+FP)}$

6 Experimental results and discussion

The Proposed clustering method was evaluated on a PC, i5 processor. Utilizing MATLAB 18.0, the clustering procedure was completed. The Proposed method was compared to existing approaches such as FCM, EnFCM, FCM-M1, FCM-S2, FGFCM, FGFCM-s2, FGFCM-s1, and FLICM.

6.1 Results on noisy images

Initially, we experimented with noisy images from the Weizmann dataset. Here two dataset images of size (Board,400 × 400 and Flower,400 × 267) are used for the experiment. The two dataset images are shown in Figure 11(a) and Figure 12(a) respectively. The dataset images are corrupted by mixed noise (a combination of Gaussian noise and salt & pepper noise) These corrupted output images are used to calculate the accuracy of the above algorithm. figures 11(c-k) and figures 12(c-k) show the output results obtained by different segmentation algorithms.

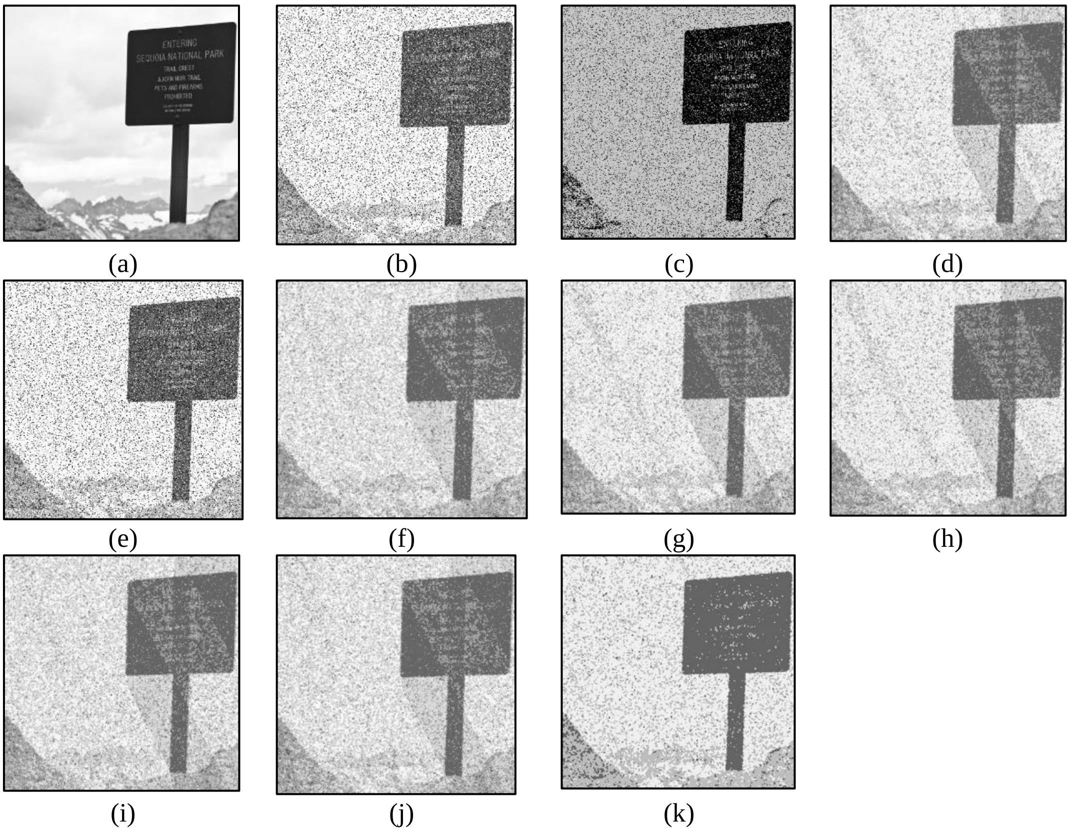

Figure 11: Comparison of output results on the Board dataset image (a) original dataset image. (b) noisy image (c) FCM (d) EnFCM (e)FCM_M1(f)FCM_S2 (g)FGFCM (h)FGFCM_S2 (i)FGFCM_S1 (j)FLICM (k)Proposed

Method.

The noise is mixed noise with zero mean and 20% variance.

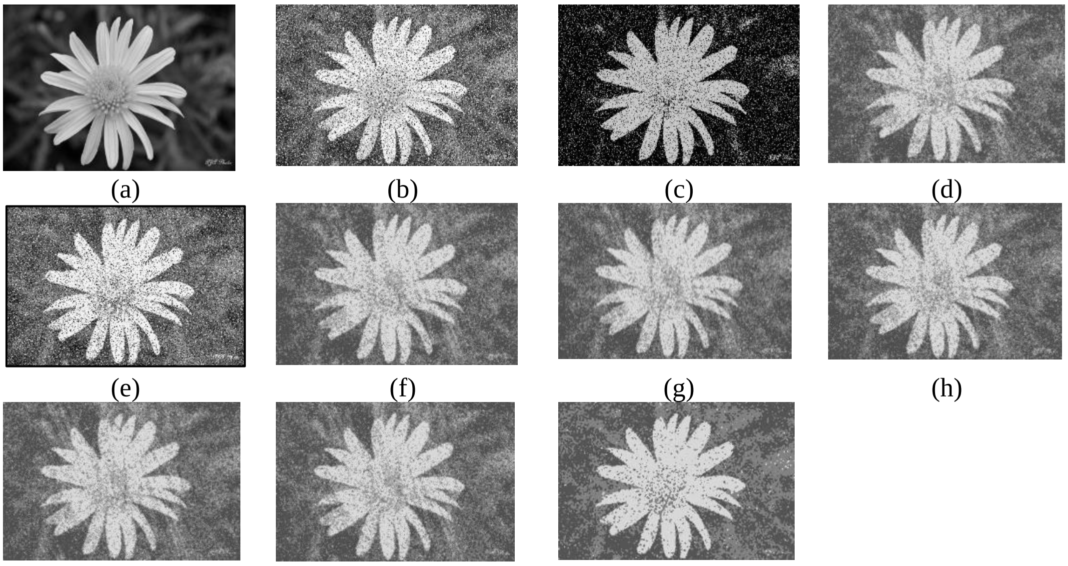

(a) (b) (c) (d)
(e) (f) (g) (h)
(i) (j) (k)

Figure 12: Segmentation results comparison on the Flower dataset image (a) Original image. (b) Noisy image (mixed noise with zero mean and 20% variance). (c) FCM (d) EnFCM (e) FCM_M1(f) FCM_S2(g) FGFCM (h) FGFCM_S2 (i) FGFCM_S1(j) FLICM (k) Proposed Method

As shown in Figure 11 FCM algorithm the segmentation result is poor. It does not overcome the sensitivity to noise. FCM_M1, the salt & pepper noise is not removed. It is affected by more noise than other methods. FGFCM and FGFCM_S2 are less sensitive to noise. The Proposed segmentation algorithm gives more accuracy than other methods.

As shown in Figure 12, the noise is not removed more in the FCM algorithm. In FCM_M1, the segmentation result is improved to some extent, and the foreground is clear. FGFCM, FGFCM_S, FGFCM_S1, and FLICM show significantly clear segmentation results. Figure 11(k) shows that the Proposed method produces superior segmentation results than previous approaches.

Table 4: Segmentation accuracy of the different algorithms on Board image with mixed noise.

Mixed Noise	FCM	ENFCM	FCM_M1	FCM_S2	FGFCM	FGFCM_S2	FGFCM_S1	FLICM	**Proposed method**
5%	91.97	91.42	93.21	91.36	90.97	90.69	91.28	91.69	**98.25**
10%	90.81	90.15	82.5	90.19	90.59	90.61	91.21	90.06	**97.86**
15%	89.29	87.3	81.53	87.82	87.01	87.45	86.72	87.23	**97.23**
20%	87.64	86.66	81.64	84.83	86.43	87.01	87.14	84.67	**96.26**
25%	85.2	87.14	81.08	86.98	86.69	84.58	86.92	86.96	**94.95**
30%	81.45	80.36	80.35	80.35	80.28	79.93	80.22	80.17	**92.53**
40%	70.55	69.84	77.67	70.41	70.01	69.57	70.42	69.89	**85.38**

Table 5: Segmentation accuracy of different algorithms on Flower image with mixed noise.

Mixed Noise	FCM	ENFCM	FCM_M1	FCM_S2	FGFCM	FGFCM_S2	FGFCM_S1	FLICM	**Proposed method**
5%	94.41	96.69	94.14	96.77	96.63	96.76	96.6	96.51	**97.93**
10%	92.14	94.6	91.46	95.03	94.75	94.46	95.00	94.58	**97.08**
15%	89.38	92.34	76.69	92.3	92.88	92.67	92.84	92.59	**96.24**
20%	86.52	89.80	69.35	89.22	90.07	90.07	89.98	89.47	**94.95**
25%	82.66	86.56	65.61	87.17	86.5	86.6	86.19	87.25	**93.06**
30%	76.97	82.75	62.54	83.02	82.69	82.81	82.75	78.14	**91.09**
40%	47.23	73.01	58.1	73.61	73.72	73.42	73.41	73.82	**85.24**

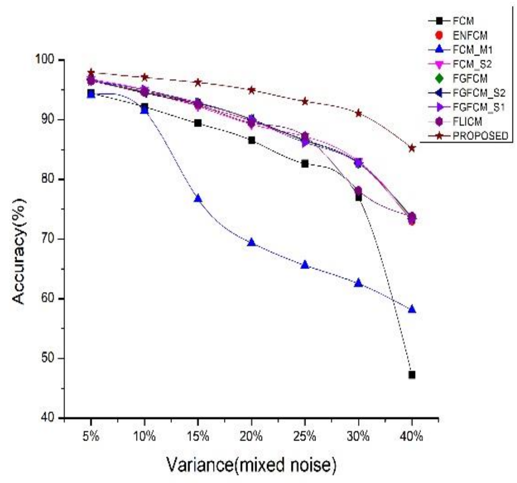

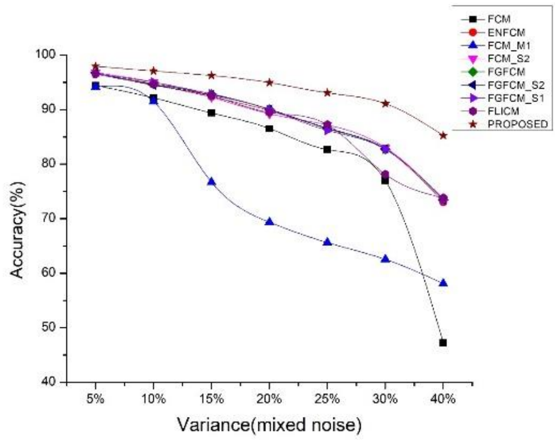

.

Figure 13: Comparison of the accuracy of nine algorithms on Board image

Figure 14: Comparison of the accuracy of nine algorithms on Flower image

To begin our study, we generated the quantitative ACC, Sensitivity, Precision, F-measure, MCC, Dice, Jaccard, and Specificity values for each image using the various techniques given in the table. Here Weizmann dataset was utilized. The best value for each statistic has been displayed for each image in bold type. The segmentation outcomes of many approaches using the Proposed method are shown in the figure.

We tested several Weizmann dataset images. One object with distinct foreground and background may be seen in each of the images. Here, we're using the suggested technique on a plain background. As demonstrated in Table 6, the Proposed method has more accuracy and specificity for the Dog image when compared to other methods. As the precision is high, it indicates that the purity of true positive identification is higher as compared to the ground truth. When the specificity is high, the amount of true negatives is accurately determined in contrast to the truth. For Bird and Flower images the precision is greater. For Eagle images, the specificity is higher in comparison to other methods. For Board images, all the parameter values are high in comparison to other methods. Hence the image is properly segmented in the Board image as shown in Figure 15. As indicated in Table 6, the parameters with the best values are bolded.

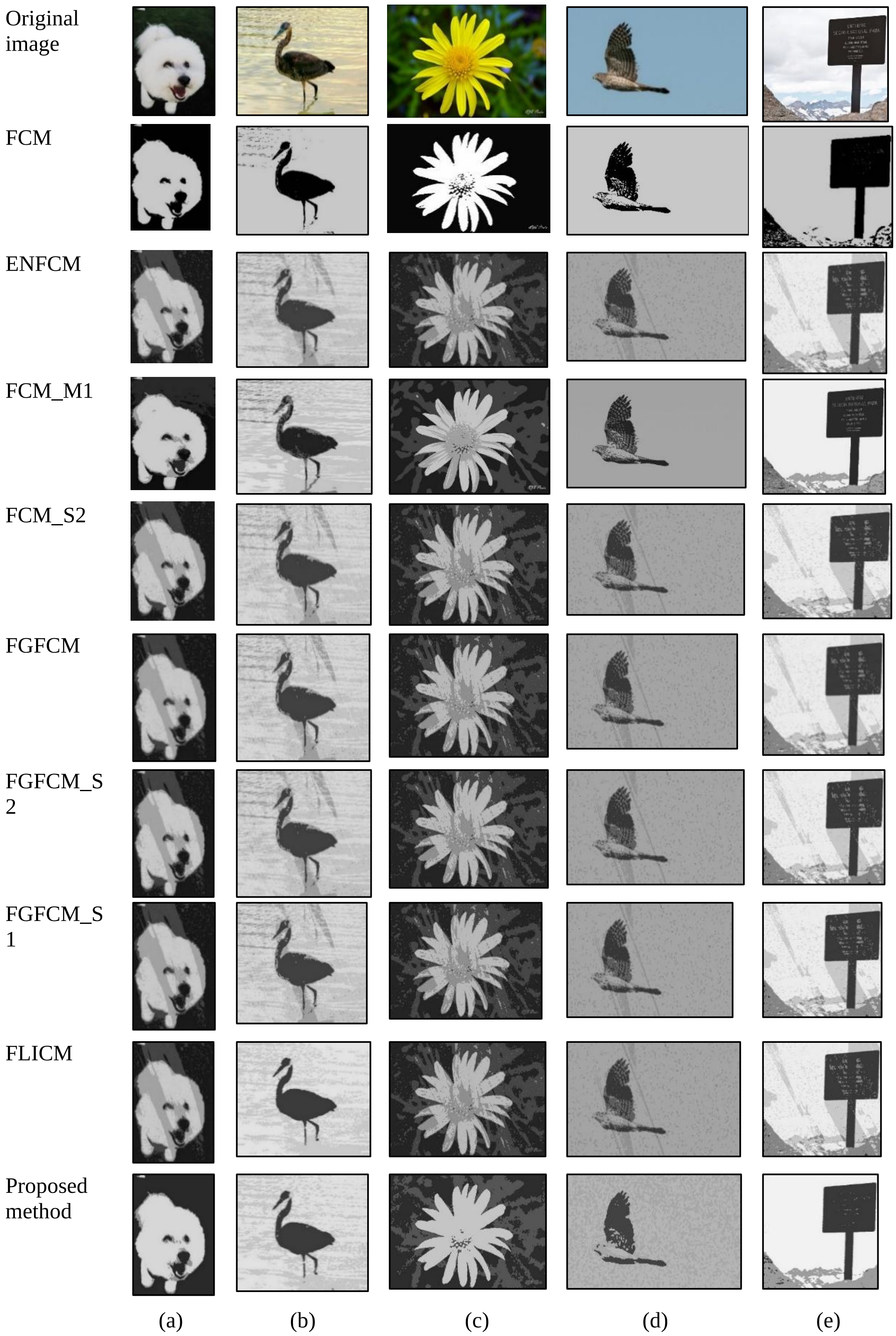

Figure 15: (a)-(e) Segmentation result of different algorithm

Table 6: Performance measure of different dataset image.

Images	Methods	Accuracy	Sensitivity	F - measure	Precision	MCC	Dice	Jaccard	Specificity
Dog	FCM	0.9221	0.9481	0.9666	0.9858	0.9624	0.9666	0.9354	0.9981
	ENFCM	0.9381	0.8876	0.9377	0.9937	0.8821	0.9377	0.8827	0.9938
	FCM_M1	0.9497	0.9108	0.9500	0.9927	0.9030	0.9500	0.9047	0.9926
	FCM_S2	0.9374	0.8864	0.9369	0.9936	0.8809	0.9369	0.8814	0.9937
	FGFCM	0.9377	0.8868	0.9372	0.9936	0.8814	0.9372	0.8818	0.9937
	FGFCM_S2	0.9376	0.8867	0.9371	0.9936	0.8812	0.9371	0.8817	0.9937
	FGFCM_S1	0.9377	0.8867	0.9372	0.9938	0.8814	0.9372	0.8819	0.9939
	FLICM	0.9381	0.8876	0.9377	0.9937	0.8822	0.9377	0.8827	0.9938
	Proposed method	**0.9572**	0.8838	0.9365	**0.9960**	0.8810	0.9365	0.8807	**0.9961**
Bird	FCM	0.9859	0.9595	0.9422	0.9256	0.9344	0.9422	0.8908	0.9895
	ENFCM	0.9837	0.8765	0.9278	0.9855	0.9206	0.9278	0.8653	0.9982
	FCM_M1	0.9837	0.8765	0.9278	0.9855	0.9206	0.9278	0.8653	0.9982
	FCM_S2	0.9007	0.9987	0.7061	0.5462	0.6956	0.7061	0.5458	0.8874
	FGFCM	0.9008	0.9989	0.7064	0.5464	0.6958	0.7064	0.5461	0.8875
	FGFCM_S2	0.8968	0.9991	0.6981	0.5364	0.6878	0.6981	0.5362	0.8829
	FGFCM_S1	0.8968	0.9991	0.6981	0.5364	0.6878	0.6981	0.5362	0.8829
	FLICM	0.8968	0.9991	0.6981	0.5364	0.6878	0.6981	0.5362	0.8829
	Proposed method	**0.9912**	0.9386	0.9623	**0.9873**	**0.9578**	**0.9623**	**0.9274**	**0.9983**
Flower	FCM	0.9878	0.9656	0.9795	0.9938	0.9710	0.9795	0.9598	0.9973
	ENFCM	0.9878	0.9656	0.9795	0.9938	0.9710	0.9795	0.9598	0.9973
	FCM_M1	0.9912	0.9871	0.985	0.9838	0.9791	0.9854	0.9713	0.9929
	FCM_S2	0.9801	0.9887	0.9679	0.9479	0.9540	0.9679	0.9378	0.9765
	FGFCM	0.9801	0.9887	0.9679	0.9479	0.9540	0.9679	0.9378	0.9765
	FGFCM_S2	0.9801	0.9887	0.9679	0.9479	0.9540	0.9679	0.9378	0.9765
	FGFCM_S1	0.9801	0.9887	0.9679	0.9479	0.9540	0.9679	0.9378	0.9765
	FLICM	0.9801	0.9887	0.9679	0.9479	0.9540	0.9679	0.9378	0.9765
	Proposed method	**0.9881**	0.9688	**0.9801**	0.9917	0.9718	**0.9801**	**0.9610**	0.9965
Eagle	FCM	0.9748	0.7653	0.8355	0.9559	0.8609	0.8655	0.7630	0.9996
	FCM_S2	0.8765	0.9547	0.6205	0.4596	0.6105	0.6205	0.4498	0.8673
	FGFCM	0.8765	0.9547	0.6205	0.4596	0.6105	0.6205	0.4498	0.8673
	FGFCM_S2	0.8765	0.9547	0.6205	0.4596	0.6105	0.6205	0.4498	0.8673
	Proposed method	**0.9812**	0.7352	0.8437	**0.9899**	0.8394	0.8437	0.7297	**0.9991**
Board	FCM	0.9392	0.9943	0.8805	0.7902	0.8505	0.8805	0.7866	0.9232
	ENFCM	0.8976	0.9994	0.8147	0.6876	0.7722	0.8147	0.6873	0.8680
	FCM_M1	0.8571	0.9998	0.7592	0.6119	0.7064	0.7592	0.6119	0.8157
	FCM_S2	0.8976	0.9994	0.8147	0.6876	0.7722	0.8147	0.6873	0.8680
	FGFCM	0.8976	0.9994	0.8147	0.6876	0.7722	0.8147	0.6873	0.8680
	FGFCM_S2	0.8976	0.9994	0.8147	0.6876	0.7722	0.8147	0.6873	0.8680
	FGFCM_S1	0.8976	0.9994	0.8147	0.6876	0.7722	0.8147	0.6873	0.8680
	FLICM	0.8976	0.9994	0.8147	0.6876	0.7722	0.8147	0.6873	0.8680
	Proposed method	**0.9903**	0.9802	**0.9786**	**0.9771**	**0.9724**	**0.9786**	**0.9582**	**0.9933**

7 Advantages and Limitations

The advantages and limitations of the method developed are highlighted below.

Advantages

(i) The developed method uses normal shrink which suppresses all kinds of noise
(ii) The method can preserve edges and fine details after the pre-processing stage
(iii) The processing time of membership filtering is less as the time requirement for each iteration is less
(iv) Misclassified pixels are detected and filtered effectively thereby resulting in better segmentation accuracy

Limitations

(i) Cluster centers are determined manually

8 Conclusion

A robust approach for improved segmentation results and to lessen the impact of noise has been suggested in this research. The normal shrink denoising algorithm is used to suppress noise of any kind. To preserve the image details and spatial information, membership filtering is used. The Proposed method produces superior segmentation outcomes for various gray-scale images according to experimental results.

References

[1] B. Wang and Z. Tu, “Affinity learning via self-diffsion for image segmentation and clustering,” in Proc. IEEE Conf. Comput. Vis. Pattern Recognit. (CVPR), Providence, RI, 2012, pp. 2312-2319.

[2] S. Kim, C. D. Yoo, S. Nowozin and P. Kohli, “Image segmentation using higher-order correlation clustering,” IEEE Trans. Pattern Anal. Mach. Intell., vol. 36, no. 9, pp. 1761-1774, Sept. 2014.

[3] A. Javed, Y. C. Kim, M. C. K. Khoo, S. L. D. Ward and K. S. Nayak, “Dynamic 3-D MR visualization and detection of upper airway obstruction during sleep using region-growing segmentation,” IEEE Trans. Biomed. Eng., vol. 63, no. 2, pp. 431-437, Feb. 2016.

[4] V. Grau, A. U. J. Mewes, M. Alcaniz, R. Kikinis and S. K. Warfield, “Improved watershed transform for medical image segmentation using prior information,” IEEE Trans. Med. Imag., vol. 23, no. 4, pp. 447-458, Apr. 2004.

[5] F. Masulli and S. Rovetta, “Soft transition from probabilistic to possibilistic fuzzy clustering,” IEEE Trans. Fuzzy Syst., vol. 14, no. 4, pp. 516-527, Aug. 2006

[6] D. Comaniciu and P. Meer, “Mean Shift: A robust approach toward feature space analysis,” IEEE Trans. Pattern Anal. Mach. Intell., vol. 24, no. 5, pp. 603-619, May 2002.

[7] D. Mahapatra. “Semi-supervised learning and graph cuts for consensus based medical image segmentation,” Pattern Recognit., vol. 63, pp. 700- 709, Mar. 2017.

[8] S. P. Chatzis and T. A. Varvarigou, “A fuzzy clustering approach toward hidden markov random field models for enhanced spatially constrained image segmentation,” IEEE Trans. Fuzzy Syst., vol. 16, no. 5, pp. 1351- 1361, Oct. 2008.

[9] D. Pathak, P. Krahenb ¨ uhl and T. Darrell, “Constrained convolutional ¨ neural networks for weakly supervised segmentation,” in Proc. IEEE Int. Conf. Comput. Vis. (ICCV), Santiago, 2015, pp. 1796-1804.

[10] J. C. Bezdek, R. Ehrlich and W. Full, “FCM: The fuzzy c-means clustering algorithm,” Comput. Geosci., vol. 10, no. 2-3, pp. 191-203, May 1984.

[11] M. N. Ahmed, S. M. Yamany, N. Mohamed, A. A. Farag and T. Moriarty, “A modified fuzzy c-means algorithm for bias field estimation and segmentation of MRI data,” IEEE Trans. Med. Imag., vol. 21, no. 3, pp. 193-199, Mar. 2002

[12] S. Chen and D. Zhang, “Robust image segmentation using FCM with spatial constraints based on new kernel-induced distance measure,” IEEE Trans. Syst., Man, Cybern., B, Cybern., vol. 34, no. 4, pp. 1907-1916, Aug. 2004.

[13] L. Szilagyi, Z. Benyo, S. M. Szilagyii, and H. S. Adam, “MR brain image segmentation using an enhanced fuzzy c-means algorithm,” in Proc. 25th Annu. Int. Conf. IEEE EMBS, 2003, pp. 17-21.

[14] W. Cai, S. Chen, and D. Zhang, “Fast and robust fuzzy c-means clustering algorithms incorporating local information for image segmentation,” Pattern Recognit., vol. 40, no. 3, pp. 825-838, Mar. 2007.

[15] S. Krinidis and V. Chatzis, “A robust fuzzy local information c-means clustering algorithm,” IEEE Trans. Image Process., vol. 19, no. 5, pp. 1328-1337, May 2010.

[16] M. Gong, Z. Zhou and J. Ma, “Change detection in synthetic aperture radar images based on image fusion and fuzzy clustering,” IEEE Trans. Image Process., vol. 21, no. 4, pp. 2141-2151, Apr. 2012.

[17] M. Gong, Y. Liang, S. Shi and J. Ma, “Fuzzy c-means clustering with local information and kernel metric for image segmentation,” IEEE Trans. Image Process., vol. 22, no. 2, pp. 573-584, Feb. 2013.

[18] Wang, Qingsheng, et al. "Robust fuzzy c-means clustering algorithm with adaptive spatial & intensity constraint and membership linking for noise image segmentation." *Applied Soft Computing* 92 (2020): 106318.

[19] Kaur, Prabhpreet, Gurvinder Singh, and Parminder Kaur. "An intelligent validation system for diagnostic and prognosis of ultrasound fetal growth analysis using Neuro-Fuzzy based on genetic algorithm." *Egyptian Informatics Journal* 20.1 (2019): 55-87.